

# Gas molecule adsorption in carbon nanotubes and nanotube bundles

Jijun Zhao<sup>1</sup>, Alper Buldum<sup>1</sup>, Jie Han<sup>2</sup> and Jian Ping Lu<sup>1</sup>

<sup>1</sup> Department of Physics and Astronomy, University of North Carolina at Chapel Hill, Chapel Hill, NC 27599, USA

<sup>2</sup> Eloret Corp., NASA Ames Research Center, MS 229-1, Moffett Field, CA 95051, USA

E-mail: zhaoj@physics.unc.edu and jpl@physics.unc.edu

Received 30 October 2001, in final form 4 March 2002

Published 14 March 2002

Online at [stacks.iop.org/Nano/13/195](http://stacks.iop.org/Nano/13/195)

## Abstract

We studied various gas molecules (NO<sub>2</sub>, O<sub>2</sub>, NH<sub>3</sub>, N<sub>2</sub>, CO<sub>2</sub>, CH<sub>4</sub>, H<sub>2</sub>O, H<sub>2</sub>, Ar) on single-walled carbon nanotubes (SWNTs) and bundles using first principles methods. The equilibrium position, adsorption energy, charge transfer, and electronic band structures are obtained for different kinds of SWNTs. Most molecules adsorb weakly on SWNTs and can be either charge donors or acceptors to the nanotubes. We find that the gas adsorption on the bundle interstitial and groove sites is stronger than that on individual nanotubes. The electronic properties of SWNTs are sensitive to the adsorption of certain gases such as NO<sub>2</sub> and O<sub>2</sub>. Charge transfer and gas-induced charge fluctuation might significantly affect the transport properties of SWNTs. Our theoretical results are consistent with recent experiments.

## 1. Introduction

In recent years, carbon nanotubes have been intensively studied due to their importance as building blocks in nanotechnology. The special geometry and unique properties of carbon nanotubes offer great potential applications, including nanoelectronic devices, energy storage, chemical probes and biosensors, field emission display, etc [1–4]. Gas adsorption in carbon nanotubes and nanotube bundles is an important issue for both fundamental research and technical application of nanotubes. Considerable experimental and theoretical efforts have been devoted to hydrogen storage in nanotube-based materials [5–9]. The effect of gas environment on the electronic properties of carbon nanotubes have recently attracted certain attentions [14–20]. Upon exposure to O<sub>2</sub>, NO<sub>2</sub>, or NH<sub>3</sub> gas, the electrical conductance of the semiconducting tubes are dramatically changed [14, 15]. NMR measurements reveal the effect of oxygen on density of state at Fermi level [16]. The resistance of metallic nanotube bundles decreases as gas molecules are removed from the sample [17]. In the field emission application of carbon nanotubes, the influence of various residual gases in the vacuum chamber is a critical factor for the long term stability [18, 19]. Theoretically, it was shown that the O<sub>2</sub> adsorption has a significant effect on electronic properties of small semiconducting nanotubes [20]. The adsorption of methane (CH<sub>4</sub>) gas on SWNTs and idealized

carbon slit pores at room temperature was studied by density functional calculations [29]. In this paper, we report first principles calculations on individual SWNTs and tube bundles with adsorption of variety of gas molecules including NO<sub>2</sub>, O<sub>2</sub>, NH<sub>3</sub>, N<sub>2</sub>, H<sub>2</sub>O, Ar, etc.

## 2. Computational methods

The self-consistent field (SCF) electronic structure calculations are performed based on density functional theory (DFT) with either localized basis (DMol) or plane-wave basis (CASTEP). The equilibrium geometry, adsorption energy and charge transfer are calculated by using the DMol program<sup>3</sup> [21]. In all the electron SCF calculations by the DMol package, a double numerical basis including *d*-polarization function (DND) was adopted. The density functional is treated by the local density approximation (LDA) with exchange–correlation potential parameterized by Perdew and Wang [22]. Geometry optimizations are performed with the Broyden–Fletcher–Goldfarb–Shanno (BFGS) algorithm with convergence criterion of 10<sup>−3</sup> au on the gradient and displacement, and 10<sup>−5</sup> au on the total energy and electron density. More accurate electronic band structure and electron density are

<sup>3</sup> DMol is a density functional theory (DFT) package based on an atomic basis distributed by MSI.

**Table 1.** Equilibrium height ( $h$ , defined by the distance between molecule mass centre and the centre of six-member carbon ring on graphite), adsorption energy ( $E_a$ ) of various molecules on the graphene sheet. LDA denotes current LDA calculations, exp. is the ‘best estimated’ experimental data [25].

	CO <sub>2</sub>	CH <sub>4</sub>	N <sub>2</sub>	H <sub>2</sub>	Ar
$h^{LDA}$ (Å)	3.11	3.34	3.31	2.92	3.31
$E_a^{LDA}$ (meV)	151	154	110	92	97
$h^{exp}$ (Å)	3.2	3.45	3.34	2.87	3.1
$E_a^{exp}$ (meV)	178	126	104	42	99

calculated by a SCF plane-wave pseudopotential technique (CASTEP)<sup>4</sup> [23]. The ion–electron interaction is modelled by Troullier–Martin norm-conserving nonlocal pseudopotential [24]. The energy cutoff of the plane wave basis is chosen up to 760 eV.

To check the validity of the present theoretical scheme, we have studied several well-known cases of gas molecule adsorption on the graphene sheet. In table 1, we compare our LDA results with those ‘best estimated’ experimental data given in [25]. We find that both the equilibrium distance and the adsorption energy are well reproduced by our present DFT scheme. It is well known that LDA is normally inaccurate in describing the van der Waals-like interaction. In our studies, we have also performed some nonlocal density functional calculations at generalized gradient approximation (GGA) level. As compared with the experimental results of gas adsorption on graphene, the inclusion of GGA somehow underestimates the molecule–surface interaction. Accordingly, the binding energy and the amount of charge transfer of molecule adsorption on SWNTs by GGA are also smaller than the prediction from LDA. For example, the adsorption energy and charge transfer of NH<sub>3</sub> molecule on a (5, 5) SWNT by GGA calculation are 54 meV and 0.01 e respectively, which is smaller than those from LDA (see table 2). The equilibrium tube–molecule distance 3.5 Å by GGA is also larger than LDA value as 3.0 Å. Therefore we argue that the real interaction intensity of the molecule–tube interaction might be intermediate between the LDA and GGA predictions and our major conclusions should be valid regardless the adopted approximation.

In this work, we studied both zigzag (10, 0), (17, 0) and armchair (5, 5), (10, 10) tubes. A one-dimensional periodic boundary condition is applied along tube axis. For (10, 0) and (17, 0) zigzag tubes, we use one molecule per unit cell in tube axis direction. Using one molecule per two unit cells shows no significant difference. For (5, 5) or (10, 10) tubes, due to the short unit cell length, reliable results are obtained by using one molecule per two unit cells. For individual SWNTs, intensive static calculations are carried out to obtain the binding curve (see figure 2) and to find the equilibrium tube–molecules distance for each system. Full geometrical minimizations are then performed to determine the optimal molecular orientations and distance. Different possible adsorption sites, T (top of an carbon atom), B (top of the centre of the C–C bond), C (top of the centre of the carbon hexagon) have been considered. The deformation

<sup>4</sup> CASTEP is a density functional theory (DFT) package based on plane-wave pseudopotential technique distributed by MSI.

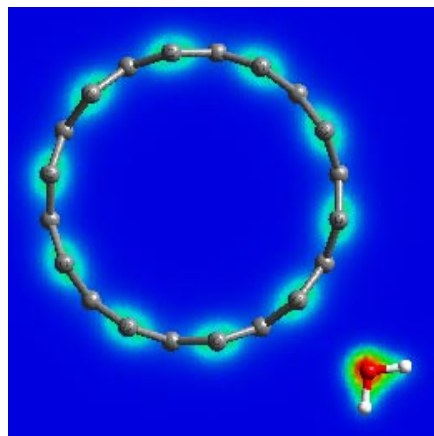


**Figure 1.** Geometric structure and total electron density (slice at (100) direction) of H<sub>2</sub>O attached to an individual (10, 0) tube. No significant overlap of the electron density is found between the molecule and tube.

of the nanotube structure upon relaxation is relatively small and does not significantly modify the electronic properties. In addition to individual SWNTs, we have also investigated the gas adsorption in the SWNTs bundle. For the (10, 10) tube bundle, we use a lattice constant 16.8 Å for the two-dimensional hexagonal lattice [26].

### 3. Results and discussions

#### 3.1. Interaction between gas molecule and an individual SWNT

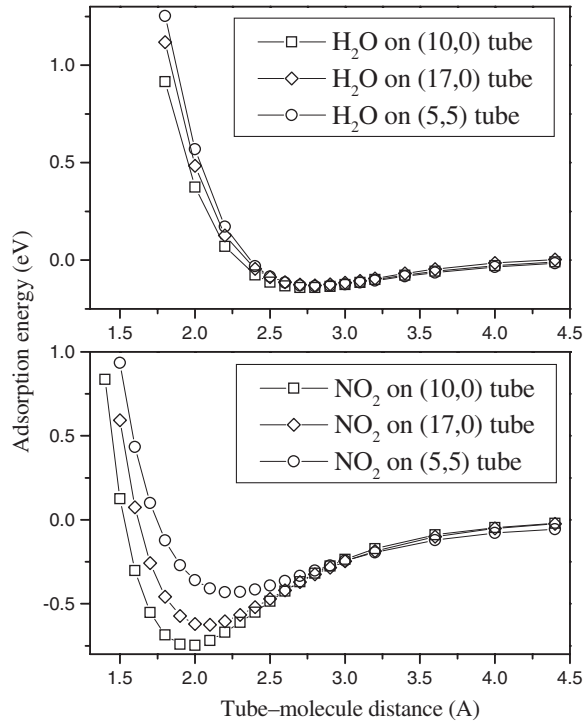
Table 2 summarizes our results on the equilibrium tube–molecule distance, adsorption energy, and charge transfer for various molecules on (10, 0), (17, 0) and (5, 5) SWNTs [18]. In general, all these gas molecules are weakly binded to the nanotube and the tube–molecule interaction can be identified as physisorption. Most molecules studied (with exception of NO<sub>2</sub> and O<sub>2</sub>) are charge donors with small charge transfer (0.01 ~ 0.035 electron per molecule) and weak binding ( $\leq 0.2$  eV). For O<sub>2</sub> and NO<sub>2</sub>, both of which are charge acceptors, the charge transfer is not negligible. This is also reflected in their larger adsorption energies.

To illustrate the tube–molecule interaction, figure 1 shows the atomic structure and total charge density of valence electrons for a H<sub>2</sub>O molecule adsorbed on (10, 0) SWNT. No substantial electron density overlap is found in the region between the gas molecule and nanotube, indicating that no chemical bond is formed. This result agrees well with a recent DMol calculation [13], which shows that the water–tube interaction is weak without electric field and can be significantly enhanced by applied field. The binding curve for H<sub>2</sub>O and NO<sub>2</sub> molecules adsorbed on (10, 0), (17, 0) and (5, 5) SWNTs are shown in figure 2. The tube–molecule interactions are comparable to the van der Waals-like interactions between these molecules and graphite surfaces [25]. Our results show that there is no clear dependence of adsorption on the tube size and chirality (table 2 and figure 2).

**Table 2.** Equilibrium tube–molecule distance ( $d$ ), adsorption energy ( $E_a$ ) and charge transfer ( $Q$ ) of various molecules on (10, 0), (17, 0) and (5, 5) individual SWNTs<sup>a</sup>. The optimal adsorption sites are given in the table: T (top of an carbon atom), B (top of the centre of the C–C bond), C (top of the centre of carbon hexagon).

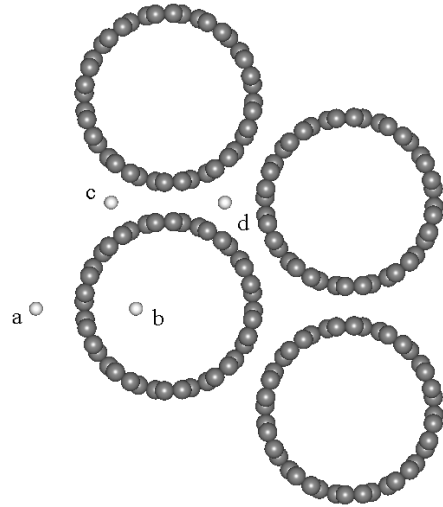
	NO <sub>2</sub>	O <sub>2</sub>	H <sub>2</sub> O	NH <sub>3</sub>	CH <sub>4</sub>	CO <sub>2</sub>	H <sub>2</sub>	N <sub>2</sub>	Ar
(10, 0) SWNT									
$d$ (Å)	1.93	2.32	2.69	2.99	3.17	3.20	2.81	3.23	3.32
$E_a$ (meV)	797	509	143	149	190	97	113	164	57
$Q$ (e)	-0.061	-0.128	0.035	0.031	0.027	0.016	0.014	0.008	0.01
Site	T	B	T	T	C	C	C	C	C
(5, 5) SWNT									
$d$ (Å)	2.16	2.46	2.68	2.99	3.33	3.54	3.19	3.23	3.58
$E_a$ (meV)	427	306	128	162	122	109	84	123	82
$Q$ (e)	-0.071	-0.142	0.033	0.033	0.022	0.014	0.016	0.011	0.011
Site	T	B	T	T	C	C	C	C	C
(17, 0) SWNT									
$d$ (Å)	2.07	2.50	2.69	3.00	3.19	3.23	2.55	3.13	3.34
$E_a$ (meV)	687	487	127	133	72	89	49	157	82
$Q$ (e)	-0.089	-0.096	0.033	0.027	0.025	0.015	0.012	0.006	0.01
Site	T	B	T	T	C	C	C	C	C

<sup>a</sup> Tube–molecule distance  $d$  is defined as the nearest distance between atoms on the molecule and the nanotube for T site, or the distance between the centre of the gas molecule and the centre of the carbon hexagon (carbon–carbon bond) for the C (B) site. The adsorption energy  $E_a(d)$  is defined as the total energy gained by molecule adsorption at equilibrium distance:  $E_a(d) = E_{tot}(\text{tube} + \text{molecule}) - E_{tot}(\text{tube}) - E_{tot}(\text{molecule})$ . Charge transfer  $Q$  denotes the total Mulliken charge number on the molecules, positive  $Q$  means charge transfer from molecule to tube.

**Figure 2.** Adsorption energy (eV) as functions of tube–molecule distance (Å) (defined as the nearest distance between the molecule and the nanotube) for H<sub>2</sub>O (above) and NO<sub>2</sub> (below) on (10, 0), (17, 0) and (5, 5) tubes.

### 3.2. Gas molecules in the tube bundle and on the bundle surface

As an example of gas adsorption in the carbon nanotube bundle, we discuss the H<sub>2</sub> molecule adsorption in the (10, 10) SWNT

**Figure 3.** Illustration of several adsorption sites for the H<sub>2</sub> molecule in the nanotube bundle. (a) Surface; (b) pore; (c) groove; (d) interstitial.

bundle. As shown in figure 3, four possible sites (surface, pore, groove, interstitial) for the H<sub>2</sub> adsorption in the tube bundle have been considered. The calculated tube–molecule distance, adsorption energy and charge transfer for the different sites are given in table 3. We find that the adsorption energy and charge transfer of H<sub>2</sub> in the interstitial and groove sites of the tube bundle are considerably larger than those on the surface sites. The pore site is also energetically more favourable than the surface site. Similar results are obtained for the other gas molecules studied. The enhancement of molecule adsorption on the groove and interstitial sites can be understood by the increased number of carbon nanotubes interacting with the molecule. Our present results compared well with a previous

**Table 3.** Equilibrium tube–molecule distance ( $d$ ), adsorption energy ( $E_a$ ) and charge transfer ( $Q$ ) of the  $H_2$  molecule on different adsorption sites (see figure 3) in the (10, 10) SWNT bundle.

Site	$d$ (Å)	$E_a$ (meV)	$Q$ (e)
Surface	3.01	94	0.014
Pore	2.83	111	0.012
Groove	3.33	114	0.026
Interstitial	3.33	174	0.035

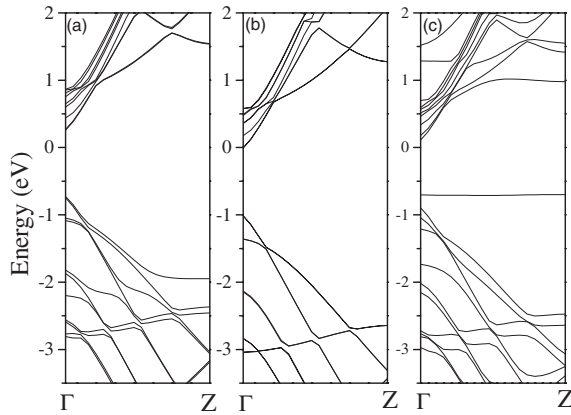


**Figure 4.** Electronic band structures near the Fermi level of (a)  $NH_3$  adsorbed, (b) pure, (c)  $NO_2$  adsorbed (10, 0) carbon nanotube. The band degeneracies in SWNT are broken by molecule adsorption. For  $NO_2$ , this effect is enhanced by the presence of a molecule level near the tube valence band edge (see also figure 6).

empirical force field simulation [10]. However, it is worth noting that the realistic possibility of adsorption of the gases other than  $H_2$  in the interstitial sites of nanotube bundles could be smaller if the kinetic radius of the gas molecule is taken into account.

### 3.3. Electronic properties of SWNT upon molecule adsorption

The electronic band structures near the Fermi level for a (10, 0) nanotube adsorbed with  $NH_3$  and  $NO_2$  are presented in figure 4 and compared with that of the pure nanotube. The band structures for either the valence or conduction bands of the carbon nanotube are not significantly changed upon the molecule adsorption. However, the degeneracies of the energy bands in SWNT are removed by the molecule–tube interaction. The band splitting cause by  $NO_2$  is more pronounced than that by  $NH_3$ . This is consistent with the larger charge transfer and the higher adsorption energy (table 2).

In figure 5, we present the electronic density of states (DOS) of individual (10, 0) SWNTs adsorbed with  $NO_2$ ,  $NH_3$ , along with that of the pure SWNT. Except for the slight modification on DOS shape due to band splitting, we find that the DOS of  $NH_3$  adsorbed nanotube is very close to that of the pure nanotube. Similar behaviour is obtained for all charge donor molecules studied ( $N_2$ ,  $H_2O$ ,  $CO_2$  etc). Therefore, we suggest that the interaction between the nanotube and these gas molecules is weak and does not have a significant influence on the electronic structures of SWNTs.

In the cases of  $NO_2$  and  $O_2$ , the interaction between molecules and SWNT are much more pronounced. As shown

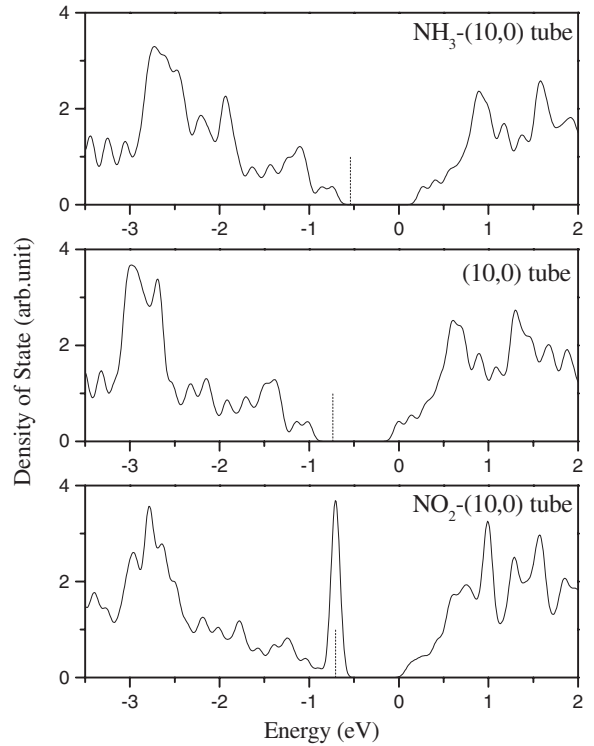


**Figure 5.** Electronic DOS corresponding to the band structures shown in figure 4. Dashed lines denote the Fermi level. 21  $k$  points are used with 0.05 eV Gaussian broadening. Modification of the DOS caused by band splitting is more pronounced in  $NO_2$  than  $NH_3$ . Due to the existence of the molecule level near the valence band edge, hybridization between SWNT and  $NO_2$  shift the Fermi level into the valence band, making SWNT a p-type conductor.

in figure 5, the adsorption of  $NO_2$  has considerably modified the shape of the DOS. Due to the existence of a half-occupied molecule level near the valence band edge, the coupling between the tube and the molecule shift the Fermi energy into the valence band and the DOS at the Fermi energy is high. Therefore, a semiconductor SWNT can be turned into p-type conductor after  $NO_2$  or  $O_2$  adsorption. Similar results have been obtained in a previous theoretical study on  $O_2$  adsorption [20].

Our present results are supported by recent experiments. For instance, the electrical conductance of an individual semiconducting tube increases dramatically upon  $NO_2$  gas exposure and the  $NO_2$  is identified as charge acceptor [14]. Collins *et al* found that the oxygen gas has dramatic effects on conductivity, thermopower, and local DOS of individual semiconductor nanotubes, while Ar, He, and  $N_2$  have no noticeable doping effect. Oxygen exposure generally converts semiconducting tubes into apparent conductors [15]. NMR experiment has further proved the increase of density of state at the Fermi level of SWNTs after exposure to oxygen [16] while most other gas like  $H_2$ ,  $CO_2$  do not have such an effect [27]. Our calculations suggest that this is probably due to the hybridization between the tube valence bands and nearby molecule levels. As suggested in [15], the air exposure effect on the measured properties of as-prepared nanotubes should be carefully examined. Many supposedly intrinsic properties

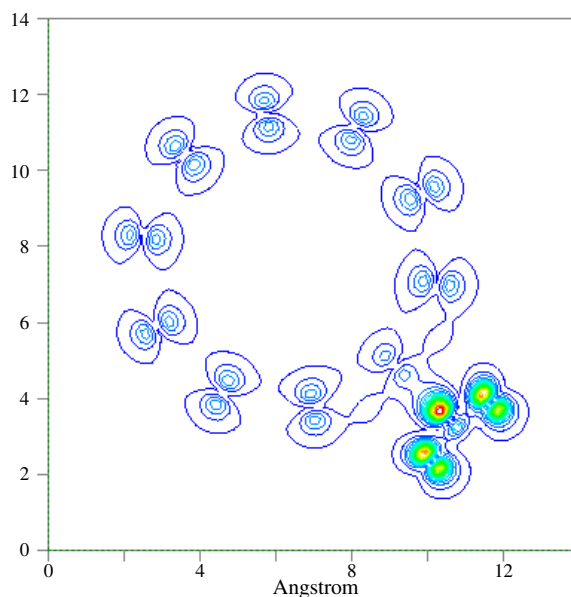


**Figure 6.** Contour plot of electron density (slice at (100) direction and passing through  $\text{NO}_2$  molecule) for the top nine valence bands. The corresponding band structures of these bands are shown in figure 5. (This figure is in colour only in the electronic version)

measured on tube samples might be severely compromised by extrinsic air exposure effects. Based on present calculations, we propose that the effects from most gas molecules in the air, such as  $\text{N}_2$ ,  $\text{CO}_2$ ,  $\text{H}_2\text{O}$ , are relatively weak. The air exposure effect should be dominated by  $\text{O}_2$ , which is a charge acceptor and make all nanotubes p-type conductors.

More insight into tube–molecule interaction can be obtained by examining the electron density. The electron density of top nine electronic bands near the valence band edge (as shown in figure 5) of  $\text{NO}_2$  adsorbed (10, 0) tube is shown in figure 6. Weak coupling between  $\text{NO}_2$  and the carbon nanotube is found. The carbon  $\pi$  bonds near the molecule are weakened due to the charge transferred from carbon to  $\text{NO}_2$ . We also find charge density redistribution on carbon close to the  $\text{NO}_2$  molecule. Therefore, we suggest that the molecule adsorption can induce a local charge fluctuation in the contact region of the nanotube. Such fluctuation may have a pronounced effect on the transport properties of metallic SWNT. The charge fluctuation can act as scattering centres for conducting electrons and increase the resistance of a metallic nanotube. In a recent experiment, it was found that the resistance of metallic tube bundles increased with gas molecules ( $\text{O}_2$ ,  $\text{N}_2$ , etc) [17]. Preliminary resistance calculations on the molecule-induced charge fluctuations found that significant resistance increase can be detected with a single molecule adsorption. A detailed study on this subject will be reported elsewhere [28].

#### 4. Conclusions

In summary, we have performed first principles calculations on the electronic properties of a nanotube upon adsorption of gas molecules. We found that all molecules are weakly adsorbed on SWNT with small charge transfer, while they can be either a charge donor or an acceptor of the nanotube.

The adsorption of some gas molecules on SWNTs can cause a significant change in electronic and transport properties of the nanotube due to the charge transfer and charge fluctuation. The molecule adsorption on the surface or inside of the nanotube bundle is stronger than that on an individual tube.

#### Acknowledgments

This work is supported by the US Army Research Office grant no DAAG55-98-1-0298, the Office of Naval Research grant no N00014-98-1-0597 and NASA Ames Research Center. The authors thank Dr X P Tang, Dr A Kleinhammes and Professor Y Wu for helpful discussions. We acknowledge computational support from the North Carolina Supercomputer Center.

#### References

- [1] Dresselhaus M S, Dresselhaus G and Eklund P C 1996 *Science of Fullerenes and Carbon Nanotubes* (New York: Academic)
- [2] Ebbesen T (ed) 1997 *Carbon Nanotube: Preparation and Properties* (Boca Raton, FL: CRC Press)
- [3] Saito R, Dresselhaus G and Dresselhaus M S 1998 *Physics Properties of Carbon Nanotubes* (New York: World Scientific)
- [4] Lu J P and Han J 1998 *Int. J. High Electron. Syst.* **9** 101
- [5] Dillon A C, Jones K M, Bekkedahl T A, Kiang C H, Bethune D S and Heben M J 1997 *Nature* **386** 377
- [6] Chen P, Wu X, Lin J and Tan K L 1999 *Science* **285** 91
- [7] Ye Y, Ahn C C, Witham C, Fultz B, Liu J, Rinzler A G, Colbert D, Smith K A and Smalley R E 1999 *Appl. Phys. Lett.* **74** 2307
- [8] Liu C, Fan Y Y, Liu M, Cong H T, Cheng H M and Dresselhaus M S 1999 *Science* **286** 1127
- [9] Wang Q Y and Johnson J K 1999 *J. Chem. Phys.* **110** 577

- Wang Q Y and Johnson J K 1999 *J. Phys. Chem. B* **103** 4809
- [10] Williams K A and Eklund P C 2000 *Chem. Phys. Lett.* **320** 352
- [11] Yin Y F, Mays T and McEnaney B 2000 *Langmuir* **16** 10 521
- [12] Lee S M and Lee Y H 2000 *Appl. Phys. Lett.* **76** 2877
- [13] Maiti A, Andzelm J, Tanpipat N and von Allmen P 2001 *Phys. Rev. Lett.* **087** 155502
- [14] Kong J, Franklin N R, Zhou C, Chapline M G, Peng S, Cho K and Dai H 2000 *Science* **287** 622
- [15] Collins P G, Bradley K, Ishigami M and Zettl A 2000 *Science* **287** 1801
- [16] Tang X P, Kleinhammes A, Shimoda H, Fleming L, Bennoune K Y, Sinha S, Bower C, Zhou O and Wu Y 2000 *Science* **288** 492
- [17] Sumanasekera G U, Adu C K W, Fang S and Eklund P C 2000 *Phys. Rev. Lett.* **85** 1096
- [18] Dean K A and Chalamala B R 1999 *Appl. Phys. Lett.* **75** 3017
- [19] Wadhawan A, Stallcup R E II and Perez J M 2001 *Appl. Phys. Lett.* **78** 108
- [20] Jhi S H, Louie S G and Cohen M L 2000 *Phys. Rev. Lett.* **85** 1710
- [21] Delley B 1990 *J. Chem. Phys.* **92** 508
- [22] Perdew J P and Wang Y 1992 *Phys. Rev. B* **45** 13244
- [23] Payne M C, Teter M T, Allen D C, Arias T A and Joannopoulos J D 1992 *Rev. Mod. Phys.* **64** 1045
- [24] Troullier N and Martins J L 1991 *Phys. Rev. B* **43** 1993
- [25] Vidali G, Ihm G, Kim H Y and Cole M W 1991 *Surf. Sci. Rep.* **12** 133 and reference therein
- [26] Lu J P 1997 *Phys. Rev. Lett.* **79** 1297
- [27] Kleinhammes A, Tang X P and Wu Y, unpublished
- [28] Buldum A, Zhao J, Lu J P and Han J, unpublished
- [29] Tanaka H, Ei-Merraoui M, Steele W A and Kaneko K 2002 *Chem. Phys. Lett.* **352** 334